Multiferroic Magnetic Sensor Based on AlN and $Al_{0.7}Sc_{0.3}N$ thin films

Yuxi Wang[*†‡], Kangfu Liu[*†‡], Shuai Shao[*†‡], Jangyong Kim[*] and Tao. Wu[*†‡‡]
Email: wangyx3@shanghaitech.edu.cn; liukf@shanghaitech.edu.cn; wutao@shanghaitech.edu.cn
[*]School of Information Science and Technology, ShanghaiTech University, Shanghai, China
[†]Shanghai Institute of Microsystem and Information Technology, Chinese Academy of Sciences, Shanghai, China
[‡]University of Chinese Academy of Sciences, Beijing, China
[‡]Shanghai Engineering Research Center of Energy Efficient and Custom AI IC, Shanghai, China

Abstract*—In this paper, multiferroic magnetic sensors based on AlN and $Al_{0.7}Sc_{0.3}N$ thin films have been studied by Finite Element Analysis (FEA). Magnetostrictive material FeGaB is utilized as the sensing element to detect external DC magnetic fields. The bilayer composite magnetoelectric structure is designed to operate at contour mode resonance in order to increase the sensitivity. A detailed description of the device model and simulated parameters are introduced. Under different DC magnetic fields, the device resonant frequency will change due to ΔE effect. Furthermore, the thickness influence of AlN and $Al_{0.7}Sc_{0.3}N$ thin films on the resonator characteristics has been analyzed.

Keywords—Multiferroic, Contour mode resonator, Magnetic sensor, COMSOL simulation

I. Introduction

Recently, the integration of multiferroic magnetic field sensors into microelectromechanical systems (MEMS) has received great attention as they are highly attractive for various applications. Generally, magnetic sensors including search coil, fluxgate, optical pumps, SQUID, Hall-effect, magneto-resistance, TMR and giant magneto-impedance[1-3]. However, applications of these devices are usually limited by low sensitivity and/or complex actuation requirements for sensing mechanisms. Multiferroic resonator composed of piezoelectric thin film and magnetostrictive thin film can be used to form magnetic field sensors, which can detect the magnetic field with ultrahigh sensitivity [2, 4, 5]. In such composite structure, the magnetostrictive and piezoelectric materials are mechanically coupled. The strain or characteristic change generated in magnetostrictive material is transferred to piezoelectric material. Therefore, additional changes in the magnetic field will lead to changes in characteristics of devices, particularly in resonant frequency, such as a series of resonators introduced in [6-8]. Furthermore, the multiferroic magnetic sensors with contour mode piezoelectric resonator has high electromechanical performance, high operate frequency and high sensitivity [9-12] .

In this work, we presented the analysis of the MEMS resonant magnetic field sensor. The bilayer composite nano-plate consists of Iron Gallium Boron (FeGaB) with wither Aluminum Nitride (AlN) or Aluminum scandium nitride ($Al_{0.7}Sc_{0.3}N$). Due to the relative high piezoelectric coefficients, CMOS compatibility and potential applications in integrated circuits, the AlN and AlScN are currently being considered as attractive alternative materials in RF front-end components [13-16]. Compared to AlN, AlScN thin film shows higher performance in piezoelectric constant, quality factors and electromechanical coupling coefficients, especially when the content of scandium is more than 20% [17-20]. And FeGaB as one of the low-loss self-biased soft magnetic films [21] has a low saturation magnetic field and a relatively high magnetostriction constant of approximately over 70 ppm [22, 23]. We incorporated these two materials into the device model to form a composite multiferroic MEMS magnetic field sensor. The characteristics of the model were analyzed by simulation.

The characteristic changes of magnetic materials caused by external magnetic fields as well as its influence on resonator devices are analyzed through finite element analysis (FEA). It is proved that the resonant frequency shift is primarily caused by magnetic field strength induced Young's Modulus change of FeGaB. This paper consists of the following parts. Section II describes the principle and mode of the introduced device. Section III simulation method includes the details of the modeling and parameters of materials. In section IV, simulation results are present and discussed. Conclusions are provided in the last section.

II. Principle and Mode

The three-dimensional (3D) structure of the presented device is shown as Fig. 1. Interdigital transducers (IDT) is employed for device resonance exciting. The piezoelectric material and magnetostrictive material form the main body of the resonator. Moreover, the magnetostrictive film transfers the electric field as a floating metal and senses the magnetic field as the sensing element. In this structure, there will be vertical electric field in the piezoelectric film to exciting and forming the resonant contour mode. Contour mode usually occurs on piezoelectric films with d_{31} parameters and generated by vertical electrical excitation. The exited contour mode usually has a good quality factor, typical over 1000. The resonant frequency, f, of the introduced device is determined by the pitch, W_0, and the resonant device parameters:

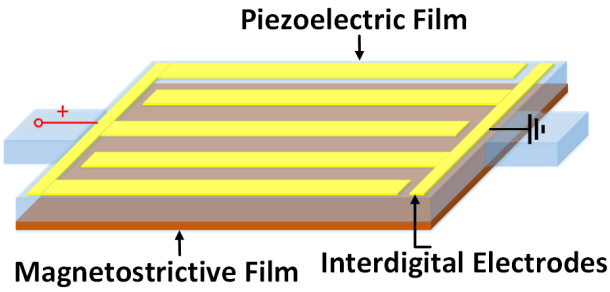

Figure 1: The model 3D structure

2021 IEEE International Ultrasonics Symposium (IUS) | 978-1-6654-0355-9/21/$31.00 ©2021 IEEE | DOI: 10.1109/IUS52206.2021.9593330

equivalent Young's Modulus E_{eq} and equivalent density ρ_{eq} by

$$f = \frac{1}{2} W_0 \sqrt{\frac{Eeq}{\rho_{eq}}} \quad (1)$$

This formula can be calculated by $E_{eq} = \sum E_i \, v_i$ and $\rho_{eq} = \sum \rho_i \, v_i$, respectively. The E_i and ρ_i is the Young's modulus and density of every single material, v_i is the volume ratio for each layer in the device.

Magnetostrictive materials exhibit a change in Young's modulus E depending on their magnetization, which is usually called ΔE effect. Equation (1) shows the mechanical resonant frequency will shift due to the changing of magnetic field. Not only the material properties will affect the characteristics of the resonator, but also the different geometric structure will bring corresponding changes, such as the change of material thickness.

III. Simulation Method

The simulation is based on the FEA software COMSOL® Multiphysics, the advantage of the software is to solve the problem of multi-physical field coupling. Two-dimensional (2D) model were built in the software, and the general schematic is shown in Fig. 2. This 2D-simulated model accurately reflects the resonator structure and also reduces calculation time. The electrode material is platinum (Pt) with a thickness t_e of 0.2 μm. The piezoelectric layer is either AlN or $Al_{0.7}Sc_{0.3}N$, and the thickness t_p is set to 1 μm. The magnetostrictive material is FeGaB, of which the thickness, t_m, is 0.1 μm. The spacing between electrode centers, W_0, is 17.5 μm.

Two physical fields are used in the simulation, one is electrostatics and the other is solid mechanics. Because the ΔE effect cannot be well simulated and characterized in finite element modeling, no additional physical field is added. We utilize the change of Young's modulus of FeGaB to represent the change of magnetic field. Some key material parameters used in the simulation are shown in Tables I and II. Table I mainly shows the basic parameters of the materials, including the thickness, density and Young's modulus of each layer. Table II is a supplement to Table I, which shows the stress-charge form of AlN and $Al_{0.7}Sc_{0.3}N$. The parameters of $Al_{0.7}Sc_{0.3}N$ in Table II can be calculated by the following formula[24]. Moreover, due to the crystal structure characteristics of $Al_{0.7}Sc_{0.3}N$, some parameters have symmetry.

$$\begin{aligned} c_{11}^E &= 410.2(1-x) + 295.3x - 210.3x(1-x), \\ c_{12}^E &= 142.4(1-x) + 198.6x - 61.9x(1-x), \\ c_{13}^E &= 110.1(1-x) + 135.5x - 78.9x(1-x), \\ c_{33}^E &= 385.0(1-x) - 23.8x - 101.4x(1-x), \\ c_{44}^E &= 122.9(1-x) + 169.5x - 137.3x(1-x). \end{aligned} \quad (2)$$

in which x means the content of Sc in $Al_{1-x}Sc_xN$ and the unit of the Young's Modulus is given in GPa. FeGaB is a magnetostrictive and conductive material, which serves as a floating metal and magnetic field sensing element in the multiferroic sensor. The ΔE effect in FeGaB means that the overall performance of the resonator will change under the influence of DC magnetic field. The change value of Young's modulus that we used is from [25], which is used to represent the change of DC magnetic field. The varying frequency responses had been studied and analyzed under different external DC magnetic fields ranging from -30 Oe to 30 Oe. In this range, the change of FeGaB properties is most obvious.

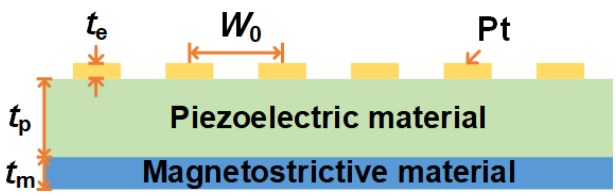

Figure 2: Two-dimensional model for simulation

IV. Results

The resonant mode shape of our presented device is shown in Fig. 3 (a). It shows contour mode of multiferroic bilayer resonator structure. The main body stretches and shrinks periodically to form a contour-shape Lamb wave. The wavelength of this resonator is 23 μm, which is twice of the spacing between two electrode centers. Fig. 3 (b) shows the simulated admittance using the initial material parameters which are listed in in Tables I and II. The resonant frequency is 342.15 MHz for $Al_{0.7}Sc_{0.3}N$/FeGaB composite resonator,

TABLE I. Simulation Parameters

Materials	Parameters		
	Thickness (μm)	*Density (kg/m³)*	*Young's modulus (GPa)*
AlN	1	3300	Anisotropy
$Al_{0.7}Sc_{0.3}N$	1	3319	Anisotropy
FeGaB	0.1	7860	215
Pt	0.2	21450	168

TABLE II. Stress-charge form of AlN and $Al_{0.7}Sc_{0.3}N$

Parameters	Value (GPa)	
	AlN	*$Al_{0.7}Sc_{0.3}N$*
c_{11}^E	410	327.7
$c_{12}^E = c_{21}^E$	149	146.9
$c_{13}^E = c_{31}^E$	99	135.4
$c_{14}^E, c_{15}^E, c_{16}^E = c_{41}^E, c_{51}^E, c_{61}^E$	0	0
c_{22}^E	410	327.7
$c_{23}^E = c_{32}^E$	99	135.4
$c_{24}^E, c_{25}^E, c_{26}^E = c_{42}^E, c_{52}^E, c_{62}^E$	0	0
c_{33}^E	389	232.1
$c_{34}^E, c_{35}^E, c_{36}^E = c_{43}^E, c_{53}^E, c_{63}^E$	0	0
c_{44}^E	125	107.9
$c_{45}^E, c_{46}^E = c_{54}^E, c_{64}^E$	0	0
c_{55}^E	125	107.9
c_{56}^E	0	0

and is 412.35 MHz for AlN/FeGaB composite resonator, respectively. The differences between the two composite resonators is attributed to various material properties and effective resonant frequencies in (1).

The magnetic field is from -30 Oe to 30 Oe, and the simulated results is shown in Fig. 4. Results show that the resonant frequency of the whole resonator will shift as the magnetic field changes. Approximately, the frequency shift increases from 0 Oe and reaches a maximum value at 14 Oe, due to the decrease of Young's modulus of FeGaB. Then, the frequency shift decreases from 14 Oe until the frequency shift basically reaches saturation after 30 Oe. The trend is also consistent with the change of Young's modulus of FGB under magnetic field. This is also consistent with the change trend of Young's modulus of FGB under external magnetic field. Due to the symmetric properties of magnetostrictive FeGaB film, the change trend from 0 Oe to -30 Oe is similar to that from 0 Oe to 30 Oe.

The maximum frequency shift of $Al_{0.7}Sc_{0.3}N$ composite resonator is 8 MHz, and the maximum frequency shift of AlN/FeGaB composite resonator is 6.9 MHz. The frequency shifts of $Al_{0.7}Sc_{0.3}N$/FeGaB composite resonator show larger value than the shifts of AlN/FeGaB composite resonator because the overall Young's modulus of $Al_{0.7}Sc_{0.3}N$/FeGaB is smaller than that of AlN/FeGaB. Similarly, from (1), the influence caused by ΔE effect in FeGaB for $Al_{0.7}Sc_{0.3}N$ composite resonator is greater than the AlN resonator.

Moreover, the thickness ratio as one of the parameters of geometry significantly affect the characteristics of bilayer resonator. We selected the magnetic field at 14 Oe which has the largest change of Young's modulus for analysis. Fig. 5(a) shows the value of frequency shift as a function of the piezoelectric layer thickness in the multiferroic composite resonator. In general, the frequency shift increases with the decrease of piezoelectric material thickness. The blue solid line is the frequency shift of the AlN/FeGaB resonator, and the maximum value is 22.9 MHz at AlN thickness of 0.1 μm. The red solid line is the frequency shift of the

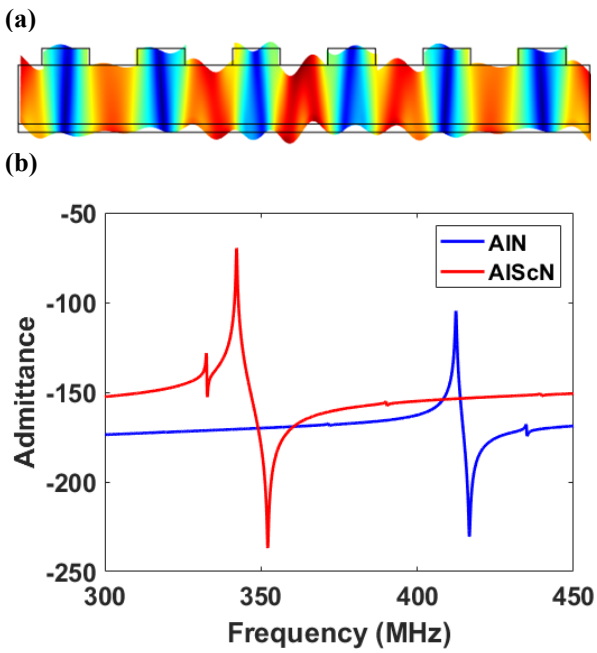

Figure 3: (a) The resonant mode and (b) the admittance of AlN composite resonator and $Al_{0.7}Sc_{0.3}N$ composite resonator.

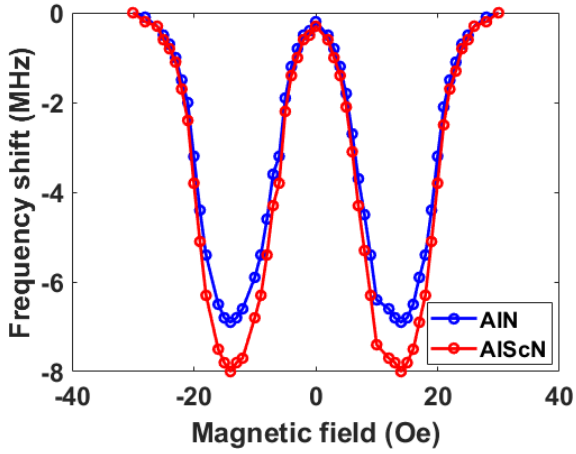

Figure 4: Frequency shift with different magnetic field.

$Al_{0.7}Sc_{0.3}N$/FeGaB resonator, which also reaches a maximum value of 25.2 MHz at the $Al_{0.7}Sc_{0.3}N$ thickness of 0.1 μm. Four different thickness (0.1 μm, 0.4 μm, 0.8 μm, 1 μm) of piezoelectric materials $Al_{0.7}Sc_{0.3}N$ are selected for further analysis of the resonance in response to the external magnetic fields. As shown in Fig. 5 (b), the magnetic field ranges from 0 Oe to 14 Oe. In this region, the magnetic field linearity is

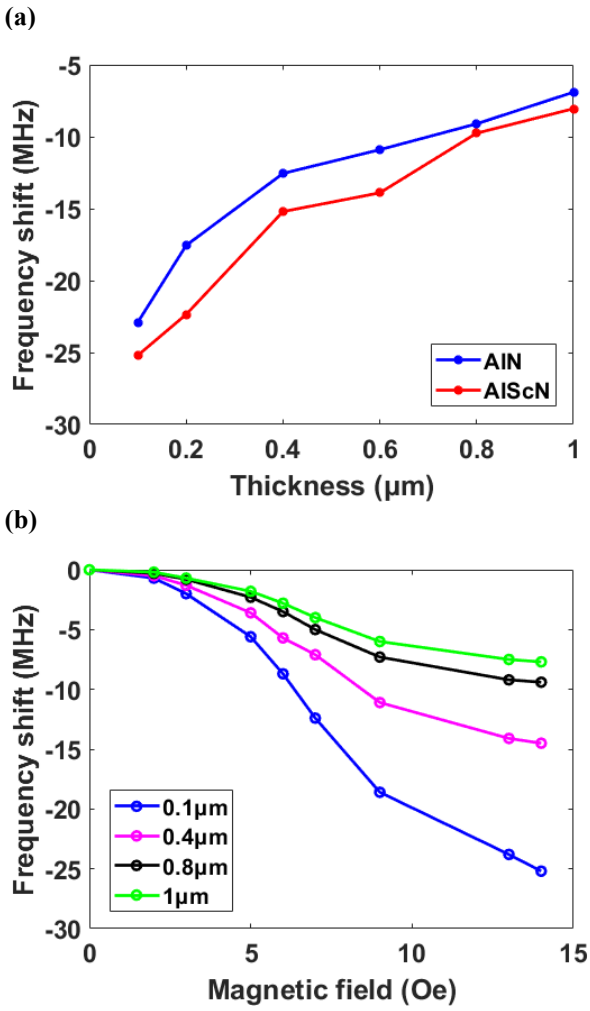

Figure 5: (a) Thickness vs frequency shift from 0.1 μm to 1 μm, and (b) Magnetic field vs frequency shift for $Al_{0.7}Sc_{0.3}N$ composite resonator of different thickness.

relatively high, especially in the range of 5 Oe to 9 Oe. For $Al_{0.7}Sc_{0.3}N$/FeGaB composite resonator with a thickness of 0.1 μm, the sensitivity of the magnetic field sensor is approximately 4.2 MHz/Oe. It indicates that the multiferroic magnetic sensor can be used to detect extremely weak magnetic field.

V. Conclusion

In summary, we have developed a model for multiferroic magnetic sensors based on FeGaB and AlN or $Al_{0.7}Sc_{0.3}N$ thin films, and compared the device performance between these two designs. The $Al_{0.7}Sc_{0.3}N$ based contour mode sensor shows higher frequency shift than that of AlN in response to the external magnetic field. The maximum value of the frequency shift, is 8 MHz for $Al_{0.7}Sc_{0.3}N$/FeGaB composite resonator and is 6.9 MHz for AlN/FeGaB composite resonator at the thickness of 1 μm. As the thickness of piezoelectric film decreases from 1 μm to 0.1 μm, the frequency shift will increase due to the thickness ratio change in the bilayer structure. The frequency shift in response to external magnetic field reaches the maximum at 0.1 μm for both device designs. Finally, the $Al_{0.7}Sc_{0.3}N$/FeGaB multiferroic sensor has demonstrated a high sensitivity of 4.2 MHz/Oe with proper magnetic bias and optimized design. The analysis of these two different materials are helpful for the development of multiferroic MEMS magnetic sensor utilizing new materials.

Acknowledgment

This work was supported from the Natural Science Foundation of Shanghai (19ZR1477000) and National Natural Science Foundation of China (61874073).

References

[1] J. Lenz, and S. Edelstein, "Magnetic sensors and their applications," IEEE Sensors Journal, vol. 6, no. 3, pp. 631-649, 2006.

[2] M. Li, A. Matyushov, C. Dong, H. Chen, H. Lin, T. Nan, Z. Qian, M. Rinaldi, Y. Lin, and N. X. Sun, "Ultra-sensitive NEMS magnetoelectric sensor for picotesla DC magnetic field detection," Applied Physics Letters, vol. 110, no. 14, pp. 143510, 2017.

[3] Y. Wang, J. Li, and D. Viehland, "Magnetoelectrics for magnetic sensor applications: status, challenges and perspectives," Materials Today, vol. 17, no. 6, pp. 269-275, 2014.

[4] Y. Hui, T. X. Nan, N. X. Sun, and M. Rinaldi, "MEMS resonant magnetic field sensor based on an AlN/FeGaB bilayer nano-plate resonator," in 2013 IEEE 26th International Conference on Micro Electro Mechanical Systems (MEMS), 2013, pp. 721-724.

[5] N. Yoshizawa, I. Yamamoto, and Y. Shimada, "Magnetic field sensing by an electrostrictive/magnetostrictive composite resonator," IEEE Transactions on Magnetics, vol. 41, no. 11, pp. 4359-4361, 2005.

[6] V. Röbisch, E. Yarar, N. O. Urs, I. Teliban, R. Knöchel, J. McCord, E. Quandt, and D. Meyners, "Exchange biased magnetoelectric composites for magnetic field sensor application by frequency conversion," Journal of Applied Physics, vol. 117, no. 17, pp. 17B513, 2015.

[7] B. Gojdka, R. Jahns, K. Meurisch, H. Greve, R. Adelung, E. Quandt, R. Knöchel, and F. Faupel, "Fully integrable magnetic field sensor based on delta-E effect," Applied Physics Letters, vol. 99, no. 22, pp. 223502, 2011.

[8] T. C. Leichle, M. v. Arx, and M. G. Allen, "A micromachined resonant magnetic field sensor," in Technical Digest. MEMS 2001. 14th IEEE International Conference on Micro Electro Mechanical Systems (Cat. No.01CH37090), 2001, pp. 274-277.

[9] S. Shao, Z. Luo, and T. Wu, "Design and Fabrication of LAMB Wave Resonator Based on 15% Scandium-Doped Aluminum Nitride Thin Film," in 2021 21st International Conference on Solid-State Sensors, Actuators and Microsystems (Transducers), 2021, pp. 1371-1374.

[10] S. Shao, Z. Luo, and T. Wu, "High Figure-of-Merit Lamb Wave Resonators Based on Al0.7Sc0.3N Thin Film," IEEE Electron Device Letters, vol. 42, no. 9, pp. 1378-1381, 2021.

[11] G. Piazza, P. J. Stephanou, and A. P. Pisano, "Piezoelectric Aluminum Nitride Vibrating Contour-Mode MEMS Resonators," Journal of Microelectromechanical Systems, vol. 15, no. 6, pp. 1406-1418, 2006.

[12] M. Rinaldi, C. Zuniga, C. Zuo, and G. Piazza, "Super-high-frequency two-port AlN contour-mode resonators for RF applications," IEEE Transactions on Ultrasonics, Ferroelectrics, and Frequency Control, vol. 57, no. 1, pp. 38-45, 2010.

[13] Z. Luo, S. Shao, and T. Wu, "Characterization of AlN and AlScN film ICP etching for micro/nano fabrication," Microelectronic Engineering, vol. 242-243, pp. 111530, 2021.

[14] A. Ding, L. Kirste, Y. Lu, R. Driad, N. Kurz, V. Lebedev, T. Christoph, N. M. Feil, R. Lozar, T. Metzger, O. Ambacher, and A. Žukauskaitė, "Enhanced electromechanical coupling in SAW resonators based on sputtered non-polar Al0.77Sc0.23N 11 2 ¯ 0 thin films," Applied Physics Letters, vol. 116, no. 10, pp. 101903, 2020.

[15] S. Barth, H. Bartzsch, D. Glöß, P. Frach, T. Modes, O. Zywitzki, G. Suchaneck, and G. Gerlach, "Magnetron sputtering of piezoelectric AlN and AlScN thin films and their use in energy harvesting applications," Microsystem Technologies, vol. 22, no. 7, pp. 1613-1617, 2016.

[16] S. Barth, H. Bartzsch, D. Gloess, P. Frach, T. Herzog, S. Walter, and H. Heuer, "Sputter deposition of stress-controlled piezoelectric AlN and AlScN films for ultrasonic and energy harvesting applications," IEEE Transactions on Ultrasonics, Ferroelectrics, and Frequency Control, vol. 61, no. 8, pp. 1329-1334, 2014.

[17] C. S. Sandu, F. Parsapour, S. Mertin, V. Pashchenko, R. Matloub, T. LaGrange, B. Heinz, and P. Muralt, "Abnormal Grain Growth in AlScN Thin Films Induced by Complexion Formation at Crystallite Interfaces," physica status solidi (a), vol. 216, no. 2, pp. 1800569, 2019.

[18] S. Leone, J. Ligl, C. Manz, L. Kirste, T. Fuchs, H. Menner, M. Prescher, J. Wiegert, A. Žukauskaitė, R. Quay, and O. Ambacher, "Metal-Organic Chemical Vapor Deposition of Aluminum Scandium Nitride," physica status solidi (RRL) – Rapid Research Letters, vol. 14, no. 1, pp. 1900535, 2020.

[19] Z. Luo, S. Shao, and T. Wu, "Optimization of AlN and AlScN Film ICP Etching," in 2021 IEEE 34th International Conference on Micro Electro Mechanical Systems (MEMS), 2021, pp. 638-641.

[20] S. Shao, Z. Luo, and T. Wu, "Optimization of S1 Lamb wave resonators with A10.8Sc0.2N," in 2021 IEEE 16th International Conference on Nano/Micro Engineered and Molecular Systems (NEMS), 2021, pp. 1523-1526.

[21] K. Yadagiri, and T. Wu, "The thickness of buffer layer and temperature dependent magneto dynamic properties of Ta/FeGaB/Ta tri-layer," Journal of Magnetism and Magnetic Materials, vol. 515, pp. 167277, 2020.

[22] J. Lou, R. E. Insignares, Z. Cai, K. S. Ziemer, M. Liu, and N. X. Sun, "Soft magnetism, magnetostriction, and microwave properties of FeGaB thin films," Applied Physics Letters, vol. 91, no. 18, pp. 182504, 2007.

[23] J. Lou, M. Liu, D. Reed, Y. Ren, and N. X. Sun, "Giant Electric Field Tuning of Magnetism in Novel Multiferroic FeGaB/Lead Zinc Niobate–Lead Titanate (PZN-PT) Heterostructures," Advanced Materials, vol. 21, no. 46, pp. 4711-4715, 2009.

[24] R. Matloub, M. Hadad, A. Mazzalai, N. Chidambaram, G. Moulard, C. S. Sandu, T. Metzger, and P. Muralt, "Piezoelectric Al1−xScxN thin films: A semiconductor compatible solution for mechanical energy harvesting and sensors," Applied Physics Letters, vol. 102, no. 15, pp. 152903, 2013.

[25] C. Dong, M. Li, X. Liang, H. Chen, H. Zhou, X. Wang, Y. Gao, M. E. McConney, J. G. Jones, G. J. Brown, B. M. Howe, and N. X. Sun, "Characterization of magnetomechanical properties in FeGaB thin films," Applied Physics Letters, vol. 113, no. 26, pp. 262401, 2018.